Chapter III

Microengineered human blood vessel to study microvascular destabilization *in vivo*

Abidemi Junaid, Wendy Stam, Sophie Dólleman, Vincent van Duinen, Hetty de Boer, Cees van Kooten, Alireza Mashaghi, Janine van Gils, Thomas Hankemeier, Anton Jan van Zonneveld

Manuscript to be submitted (2020)

Abstract

Vascular diseases are one of the main causes of mortality in the world. The development of models that effectively recapitulate the human vasculature is essential for studying the pathogenesis and therapeutic approaches for vascular diseases. Here we describe the development of a perfusable microvessel-on-a-chip featuring the human endothelium that is partly surrounded with extracellular matrix (ECM). The system is high-throughput, which allows parallel analysis of organ-level microvessel pathophysiology *in vitro*. Exposure of the microvessels to VEGF, histamine and TNFα led to albumin leakage, reconstituting the vascular leakage seen *in vivo*. Moreover, we demonstrated that this process involves changes in cellular mechanics. Finally, we developed a method to screen blood samples with our platform. Plasma samples were prepared from whole blood and treated with hirudin, corn trypsin inhibitor (CTI) and compstatin. Subsequently, this plasma cocktail was spiked with VEGF, histamine and TNFα and perfused in the microvessels-on-chips, which showed increase in vessel permeability. Our study confirms the effect of destabilizing factors in blood to induce vascular leakage in a physiological relevant *in vitro* setting. We anticipate our assay to serve as a unique tool for microvascular destabilization studies as well as for the development of novel therapeutic strategies to combat vascular diseases.

Introduction

For centuries, vascular diseases produced massive health and economic burdens globally [1]. One of the most crucial functional units of the vascular system are the endothelial cells. They are involved in coagulation of blood, inflammation, hemodynamic, signal transduction and semi-selective barrier. Endothelial dysfunction is a key factor for vascular diseases [2].

As current human 2D models with cultured endothelial cells lack sufficient complexity to assess the functionality of the microvascular system, research on microvascular loss largely depends on pre-clinical animal models for ischemia and reperfusion injury. However, animal models occasionally show an inexact representation of vascular diseases and disorders, because the anatomy, immune systems and inflammatory responses of animal microvessels differ considerably from those in humans [3]. This imperfection leads to failure in predicting efficacy, safety and toxicity of chemicals in humans, which then causes a devastating blow in clinical trial failures [4, 5].

Organs-on-Chips have recently emerged as a new research method to mimic the activities, mechanics and physiological responses of human organ systems. These microsystems can be embedded with a particular disease [6-8]. Moreover, they offer new possibilities for increasing the speed and accuracy of drug testing [9]. Extensive research has shown positive feasibility in using these 3D microfluidic models to create perfusable microvessels for investigating endothelial barrier function [10-12]. Although there are many organs-on-chips on the market that model microvessels, most of these models unfortunately depend on using cell culture media to investigate vascular permeability [13]. To better mimic vascular diseases and disorders, a more reasonable option is to perfuse 3D modelled microvessels with human blood plasma. This is of great importance because plasma contains plethora of circulating markers that regulate cell viability. For example, circulating markers in chronic kidney disease, such as tumor necrosis factor alpha (TNFα) and Interleukin 6 (IL-6) induce systemic inflammatory state and endothelial activation. This results in endothelial cell activation associated with the shedding of components of the glycocalyx, adhesion molecules and endothelial microparticles into the systemic circulation. The process ends with the detachment of endothelial cells accompanied with vascular leakage and heart failure [2, 14, 15].

To investigate the aspects of endothelial function in vascular disease models, we micro-engineered a microfluidics-based, 3D microvessel-on-a-chip platform that mimics human microvessels. Our system allows quantitative and parallel testing of microvascular leakage. Moreover, we developed an approach to screen human blood plasma in the microvessel-on-a-chip for the presence of circulating markers of endothelial activation.

Materials and Methods

Chip design

We designed a novel chip structure (T-design) based on the MIMETAS OrganoPlate platform. This new design involves a T-junction shown in Figure 1 in which the channels are separated by a phaseguide. The design, due to its geometry, enables easy generation of leak tight vessels and quantification of vascular leakage. Fabrication of the glass chipsets was carried out by MIMETAS using a previously established protocol [36].

Cell culture

Human umbilical vein endothelial cells (HUVECs) were cultured in Endothelial Cell Growth Medium 2 (EGM2; C-39216, PromoCell). We used the T-design OrganoPlate for all microfluidic cell culture. Thus, the microvascular and extracellular matrix (ECM) channels were separated by phaseguides. Before seeding the cells, 4 mg/ml rat tail collagen type 1 (3440-005-01, Trevigen) neutralized with 10% 37 g/L Na_2CO_3 (S5761, Sigma) and 10% 1 M HEPES buffer (15630-056, Gibco) was added in the ECM channels. Subsequently, the collagen was let to polymerize by incubating the device for 10 minutes in the incubator at 37°C and 5% CO_2. The observation windows were filled with 50 µl Hank's Balanced Salt Solution with calcium and magnesium buffers (HBSS+; 24020117, Life Technologies) for optical clarity. The ECM inlets were filled with 20 µl HBSS+ to prevent gel dehydration. Cells were seeded with a density of $20 \cdot 10^6$ cells/ml in gelatin-coated microvascular channels of the OrganoPlate. Afterwards, the cells were incubated at 37°C and 5% CO_2 for one hour to allow microvascular formation. After incubation, 50 µl of medium with 50% EGM2 and 50% Pericyte Growth Medium (cAP-09B,

Angio-Proteomie) was added to the inlets and outlets of the microvascular channels. The device was placed on a rocker platform with a 7° angle of motion and an eight-minute timed operation to allow continuous flow of medium in the microvessels. After 24 h, the medium was refreshed, and the HUVECs were cultured for an additional 3-4 days.

Coagulation Tests

The prothrombin time (PT) assays and the activated partial thrombin time (aPTT) assays were performed in the STart® Line: STart Max® (Diagnostica Stago) and 25 µM compastatin (supplied by our collaborators) was used in both assays. Ethylenediaminetetraacetic acid (EDTA) platelet poor plasma (PPP) was diluted to 50% plasma in dilution media of 50% EGM2 and 50% Pericyte Growth Medium. For the PT assay, 10 µM hirudin (94581-1EA, Sigma-Aldrich) was serial diluted in 50% plasma, 50 µl of each plasma dilution was incubated at 37°C for one minute. Coagulation was initiated with 50 µl of Neoplastine Ci Plus 10 (Diagnostica Stago), 1:10 diluted with dilution medium at 37°C and clotting time was measured. For the aPTT assay, Corn Trypsin Inhibitor (CTI) 500 µg/ml (CTI-01, Haematologic Technologies, Inc.) was serial diluted in 50% plasma and 50 µl of each plasma dilution was incubated at 37°C for three minutes with 50 µl of aPTT reagent (TriniClot). Coagulation was initiated with 50 µl of 25 mM $CaCl_2$ at 37°C.

Complement assay

The complement activation product C3 was measured by classical pathway activity enzyme-linked immunosorbent assay (ELISA). Wells were coated with 2 µg/ml human IgM in coating buffer (0.1 M $NaHCO_3$, 0.1 M Na_2CO_3, pH 9.6). Plasma samples were diluted in GVB++ (Gelatin Veronal Buffer, with 1 mM $MgCl_2$, 2 mM $CaCl_2$, 0.05% Tween). The in house made monoclonal antibody RFK22, labeled with digoxigenin (DIG) in incubation buffer (PTB; PBS, 0.05% Tween, 1% BSA) was used as a capture antibody. C3 was measured by using anti-DIG-horseradish peroxidase antibody in incubation buffer (PTB; PBS, 0.05% Tween, 1% BSA). Subsequently, the samples were developed with 3,3',5,5'-Tetramethylbenzidine (TMB) substrate solution. After 15 minutes, the reaction was stopped with H_2SO_4 and the optical density (OD) was measured at 450 nm.

Plasma assay

EDTA-plasma samples were treated with 1 μM hirudin (94581-1EA, Sigma-Aldrich), 50 μg/ml CTI (CTI-01, Haematologic Technologies), 25 μM compstatin and finally recalcified with 3.1 mM $CaCl_2$. These treated plasma samples were mixed with 50% EGM2 and 50% Pericyte Growth Medium. Finally, we perfused this cocktail mix in the microvessels-on-chips.

Vascular leakage assay

Endothelial cell culture media and plasma samples of healthy controls were spiked with vascular endothelial growth factor (VEGF; 450-32, PeproTech), histamine (H7125 SIGMA, Sigma-Aldrich) and tumor necrosis factor-α (TNF-α; H8916 SIGMA, Sigma-Aldrich). To measure vessel permeability, the ECM channel inlets were refreshed with 20 μl HBSS+ buffers (Life Technologies; Bleiswijk; The Netherlands). Then, the media in the inlets and outlets of the microvascular channels were replaced with 40 μl and 30 μl of 125 μg/ml Albumin-Alexa 555 (A34786, Life Technologies). Following this, the OrganoPlate was placed in the environmental chamber (37°C; 5% CO_2) of a fluorescence microscope system (Nikon Eclipse Ti) and time-lapse images were captured.

We calculated the permeability coefficient by determining the fluorescent intensities in the microvascular channel of captured images. At the same time, the fluorescent intensities in the ECM channel of the capture images was obtained and normalized with the fluorescent intensities in the microvascular channel of each measured time point. This showed the change in intensity ratio inside the gel channel as a function of time. The scatter plot was fitted with a linear trend line to determine the slope. Finally, using Fick's First Law the apparent permeability was determined as [37, 38]:

$$P_{app}(\cdot\, 10^{-6}\ cm/s) = \frac{d\left(\frac{I_g}{I_p}\right)}{dt} \cdot \frac{A_g}{l_w}$$

where I_p is the intensity in the microvascular channel, I_g is the intensity in the ECM channel, A_g $(480 \cdot 10^{-6}\ cm^2)$ is the area of the ECM channel and l_w $(400 \cdot 10^{-4}\ cm)$ is the length of the vessel wall that separates between ECM and microvascular region. All data analysis was done with ImageJ and Matlab (2016a, MathWorks).

Transendothelial electrical resistance (TEER) measurements

Cell barrier function was assessed by measuring transendothelial electrical resistance (TEER) in real time using the Electric Cell-substrate Impedance Sensing (ECIS ZΘ, Applied BioPhysics) system. HUVECs at a density of $15 \cdot 10^3$ cells per well were dispensed and grown to a confluent monolayer on 1% gelatin-coated 96W20idf electrodes (Applied BioPhysics) in 200 µl EGM2 in a 5% CO_2 incubator at 37°C for 48 hours. For the coating, gelatin was dissolved in water. Monolayer resistance was recorded at 4 kHz over 15 minutes intervals for baseline measurement. Subsequently, 75 µl medium was taken out and 75 µl recalcified 50% EDTA-plasma with 1 µM hirudin, 50 µg/ml CTI and 25 µM compstatin was added for 6 hours before treatment. After 6 hours, 75 µl of the EDTA-plasma cocktail and medium were replaced by 75 µl of the plasma cocktail and medium spiked with VEGF, histamine and TNFα.

For analysis of changes in barrier function, TEER measurements were averaged over the last 10 stable pre-treatment time points as baseline. For the percentage resistance, TEER values were corrected for the base line.

Immunocytochemistry

The medium was aspirated from the medium inlets and outlets of the chips and cells were fixed using 4% paraformaldehyde (PFA) in HBSS+ for 10 minutes at room temperature. The fixative was aspirated and cells were rinsed once with HBSS+. Next, cells were permeabilized for two minutes with 0.2% Triton X-100 in HBSS+ and washed once with HBSS+. The cells were blocked with 5% BSA in HBSS+ for 30 minutes and incubated with primary antibody solution overnight at 4°C. Mouse anti-human CD144 (1:100; 555661, BD Biosciences) and 10H10 (supplied by our collaborators) were used as the primary antibodies. The wells were washed

with HBSS+, followed by the addition of Hoechst (1:2000; H3569, Invitrogen), rhodamine phalloidin (1:200; P1951 SIGMA, Sigma-Aldrich) and secondary antibody solution containing goat-anti-mouse Alexa Fluor 488 (1:250; R37120, Waltham). After one hour of incubation in the dark at room temperature, wells were washed three times with HBSS+. High quality Z-stack images of the stained cells were obtained using a high-content confocal microscope (ImageXpress Micro Confocal, Molecular Devices).

Statistical analysis

For statistical analyses, we used IBM SPSS Statistics 23. Values are given as mean ± SEM. Multiple comparisons were made by one-way ANOVA followed by Dunnett's t-test. Results were considered significant at *P < 0.05, **P < 0.01, ***P < 0.001.

Results

Development of a functional microvessel-on-a-chip

To construct the human microvessel-on-a-chip, we used the fabricated OrganoPlates (T-design). It is based on a 384-well microtiter plate format and employs coverslip-thickness glass (175 µm) for optical access [7]. A plate comprises microfluidic tissue chips, that can be used to establish 96 microvessels with heights of 120 µm and widths of 400 µm (Figure 1a). Each chip contains phaseguides for adjusting the capillary pressure to pattern type 1 collagen in the ECM channel (Figure 1b). The ECM channel enables diffusion-based solute flux across the endothelial monolayer that was used to measure the endothelial permeability (Figure 1e). After seeding the collagen, we cultured primary HUVECs in the perfusion channel. For easier operation of the chips, gravity-induced flow was used. Immunofluorescence confocal microscopic analysis showed that these cells formed leak-tight microvessel after five days in culture. Cell shape was maintained by F-actin. Moreover, the HUVECs were joined by adherence junctions containing VE-cadherin (Figure 1c and d). This enabled the formation of a robust endothelial barrier or leak-tight microvessel that restricted the passage of fluorescent albumin (67 kDa) between the endothelial monolayer and the ECM channel for 10 minutes

(Figure 1f and h). The endothelial barrier was disturbed with 10 nM thrombin for 20 minutes, which enabled an increase in endothelial permeability and represented vascular leakage (Figure 1g and h). Thus, our human microvessel-on-a-chip effectively recapitulated many of the structures and functions of microvessels under healthy and stressed conditions.

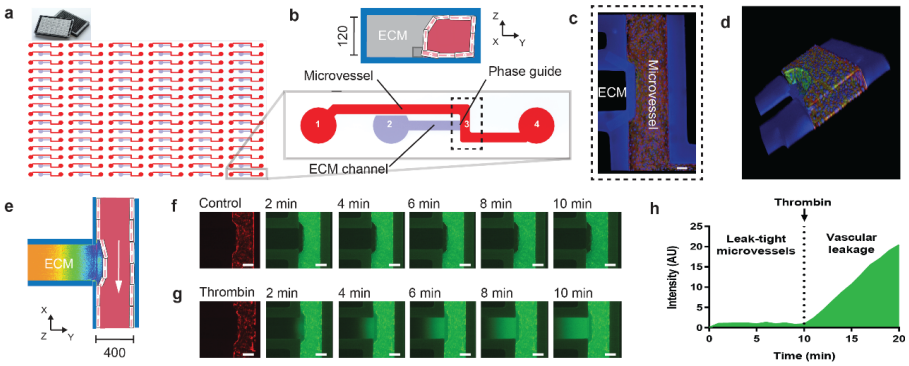

Figure 1 | The human microvessel-on-a-chip. (a) Schematic diagram of 96 microfluidic tissue chips that compromise a gradient design (T-design) in the OrganoPlate. The highlighted rectangular box shows the area depicted in **b**. **(b)** Diagram of a single chip; 1 = medium inlet, 2 = gel inlet, 3 = observation window, 4 = medium outlet. The inlay shows the compartments of the microvessel and the ECM. The dashed rectangular box highlights the region shown in **c**. **(c)** Cultured HUVECs formed (red, F-actin) a microvessel that exhibited continuous intercellular junctions on-chip, as demonstrated by VE-cadherin staining (green). Scale bar, 100 µm. **(d)** A 3D reconstruction showing the human microvessel-on-a-chip. **(e)** Fluorescent intensity profile illustrating the distribution of albumin in a 3D collagen ECM region under experimental conditions. Bluish colors indicate higher fluorescent intensities. **(f)** Time-lapse fluorescent images of albumin (green) diffusing from the microvessel (red) to the ECM channel. Scale bar, 200 µm. **(g)** Time-lapse fluorescent images of albumin (green) diffusing from the microvessel (red) to the ECM channel after treatment with 10 nM thrombin for 20 minutes. Scale bar, 200 µm. **(h)** Fluorescent intensity profile of **f** and **g**, illustrating leak-tight microvessels and vascular leakage after treatment with 10 nM thrombin. There was a sharp increase in albumin concentration across the endothelial monolayer and a steady diffusive flux inside the 3D ECM.

Modeling microvascular dysfunction on-chip

Vascular endothelial growth factor (VEGF) is known to increase leakage of plasma components by perturbing endothelial barrier integrity. VEGF activates endothelial cells by inducing phosphorylation and internalization of VE-cadherin [16, 17]. Perfusion of VEGF in our human microvessel-on-a-chip led to a dramatic increase in vessel permeability, as shown in Figure 2a and also in line with TEER measurement and other *in vitro* findings (Figure 2d) [16]. VEGF induced stress fiber formation and VE-cadherin distribution was in a zig-zag pattern with visible gaps between the cells, indicating internalization of VE-cadherin (Figure 2g).

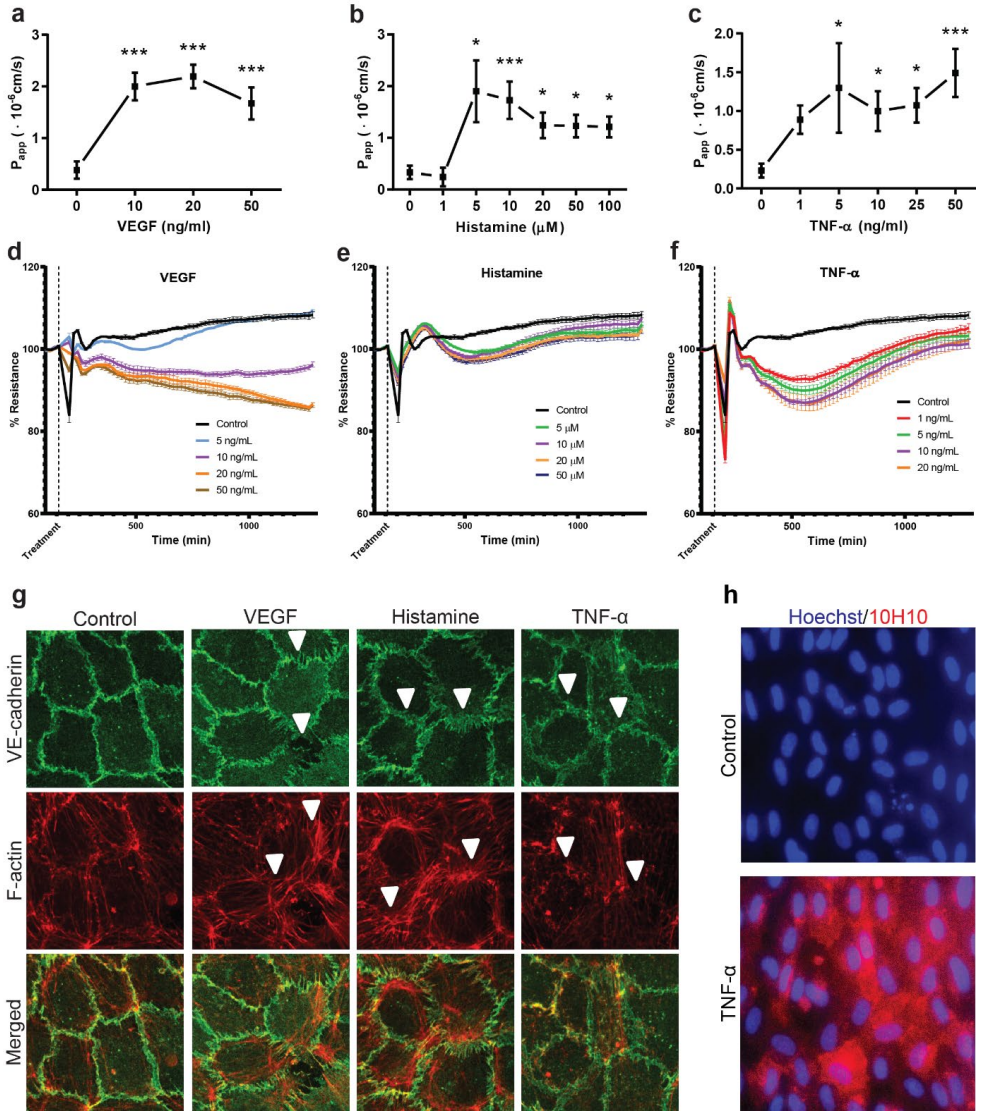

Figure 2 | Modeling microvascular dysfunction in microvessel-on-a-chip. (a) Dose response to VEGF in microvessels. Microvessels were treated for 1.5h at 37°C with several concentrations of VEGF, followed by vascular leakage assay. **(b)** Dose response to histamine in microvessels. Microvessels were treated for 1h at 37°C with several concentrations of histamine, followed by vascular leakage assay. **(c)** Concentration dependence of TNFα effect. Microvessels were treated overnight at 37°C with several concentrations of TNFα, to measure vascular leakage. Data are presented as mean and s.e.m of 3-6 biological replicates; n = 6-19 (chips). Significance determined by ANOVA and Dunnett's t-test; *P < 0.05, **P < 0.01, ***P < 0.001. **(d-f)** The effects of VEGF, histamine and TNFα on endothelial barrier function were measured in the Electric Cell-substrate Impedance Sensing (ECIS) at different doses. Data are represented as mean and s.e.m of 3-4 technical replicates. **(g)**

Microarchitecture of endothelial cells in response to 10 ng/ml VEGF (1.5h), 10 µM histamine (1h) and 10 ng/ml TNFα (overnight) showing the nucleus (blue), VE-cadherin (green) and F-actin (red). These permeability factors induced morphological rearrangement of VE-cadherin and F-actin (arrow). **(h)** Representative pictures of immunostaining of the nucleus (blue) and tissue factor (red) after treatment with 10 ng/ml TNFα (overnight).

In vivo, histamine is known as inflammatory response factor. It is a mediator of allergic inflammation that increases vascular permeability by changing VE-cadherin localization at endothelial cell junction [18]. To mimic this aspect, we modulated endothelial permeability by stimulation of the microvessels with histamine. Treatment of the microvessels with histamine increased permeability significantly (Figure 2b). The effect was further validated in the impedimetric assay, showing a drop in TEER after administration of histamine (Figure 2e). This organic compound caused increase in stress fiber formation and low distribution of VE-cadherin (Figure 2g).

Endothelial cell activation often involves the exposure of NADPH oxidase (NOX) to cytokines, such as tumor necrosis factor alpha (TNFα), which then induces oxidative stress and at the end vascular leakage of plasma fractions [2, 10]. Stimulation of the microvessels-on-chips with TNFα increased the barrier permeability progressively as we increased the concentration of the cytokine (Figure 2c). The perturbation of the endothelial barrier by TNFα was also confirmed in the ECIS system (Figure 2f). Immunostaining showed changes in VE-cadherin arrangement, actin filaments and tissue factor (TF) expression. These effects are typically seen in vascular diseases (Figure 2g and h) [19].

These results are consistent with the findings from past studies that VEGF, histamine and TNFα induce vascular leakage *in vivo* [18, 20]. They show the importance of adherens junctions in maintaining leak-tight microvessels. Moreover, our findings confirm that the human microvessel-on-a-chip can be used to investigate vascular diseases.

Perfusing human blood plasma in microvessels *in vitro*

Being able to perfuse the microvessel-on-a-chip and measure vascular leakage, our next goal was to introduce human blood plasma in the model. As recalcified EDTA-plasma is known to coagulate, we used a combination of the anticoagulants hirudin and CTI to prevent this.

Hirudin specifically binds and inhibits the activity of thrombin to convert fibrinogen into fibrin. In plasma, hirudin extended the clotting time effectively (Figure 3a). The intrinsic coagulation pathway is activated in our microfluidic system, because of the negative charge property of the glass surface. CTI is a specific human factor XIIa inhibitor and when added to plasma, it prolonged the activated partial thromboplastin time (aPTT) (Figure 3b). Besides coagulation, we suspected the appearance of complement activation in blood plasma collected from humans. To confirm this, we performed a complement activation assay for C3 deposition. Incubation of the plasma cocktail provides exceedingly high levels of C3 deposition, proving complement activation in our system. To inhibit complement activation, we used compstatin, a C3-targeted complement inhibitor [21, 22]. We observed a strong decrease of C3 deposition (Figure 3c). This result confirms that compstatin abrogates complement dysregulation in collected EDTA-plasma. By inhibiting complement activation, we can focus on biomarkers that are unique for various vascular diseases in our microvessel-on-a-chip. Immunofluorescence microscopic analysis showed that these culture conditions resulted in the formation of endothelial cells linked by VE-cadherin. The morphology of these cells was comparable to those cultured with endothelial cell culture media (Figure 3d). Perfusing the microvessels with EDTA-plasma cocktail of healthy donors maintained leak-tight vessels (Supplementary Figure 1). These results show the efficacy of the microvessel-on-a-chip with perfused human blood plasma for (pre-)clinical studies. Altogether, we have developed a high-throughput method that can be used to screen blood for markers that have impact on microvascular physiology and pathology. The first step in the process is to collect blood samples in EDTA-tubes. Subsequently, plasma samples are separated by centrifugation and treated with hirudin, CTI and compstatin. The plasma samples are perfused in the microvessels-on-chips and the permeability of these microvessels are visualized with a high-content confocal microscope and analyzed.

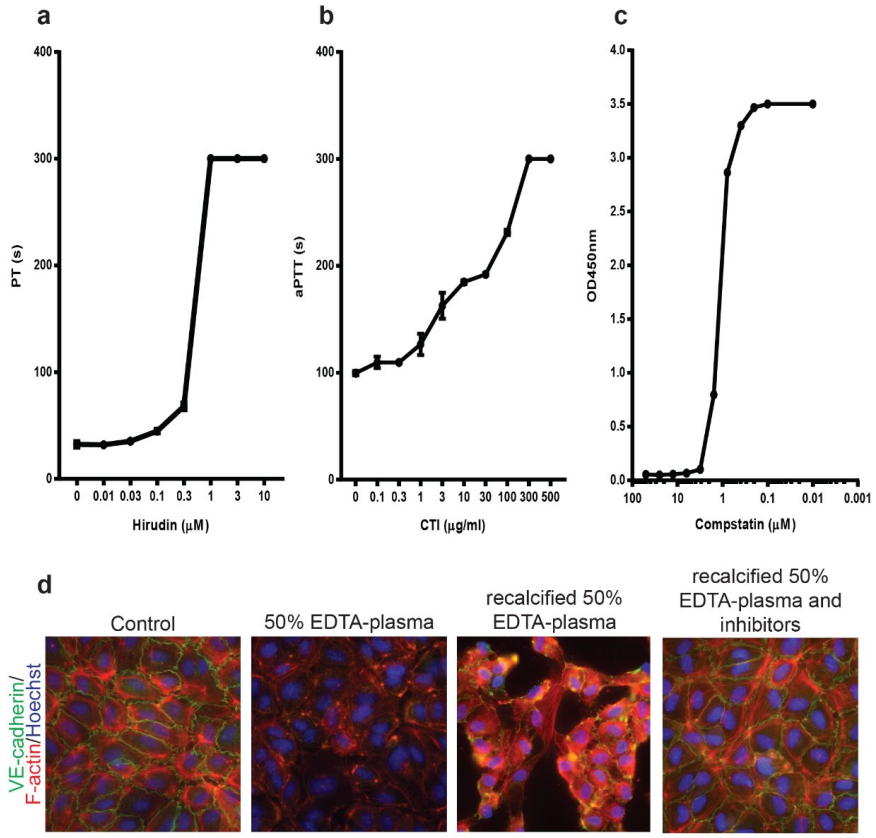

Figure 3 | Coagulation and complement inhibitors for use in EDTA-plasma *in vitro* biocompatibility models. (a) The graph illustrates the effect of added hirudin on the prothrombin time (PT) of re-calcified EDTA-plasma. **(b)** Data represents the effect of CTI on the activated partial thrombin time (aPTT) of recalcified EDTA-plasma. **(c)** Summary of the efficacy of compstatin in selectively inhibiting complement activation in recalcified EDTA-plasma. Data are presented as mean and s.e.m; n = 2 **(d)** Immunostaining of HUVECs under endothelial cell culture media (control), 50% EDTA-plasma, recalcified 50% EDTA-plasma and recalcified 50% EDTA-plasma with 1 μM hirudin, 50 μg/ml CTI and 25 μM compstatin.

As human blood plasma contains large number of factors that are major cause of vascular leakage, we next established our microfluidic model for clinical relevancy by spiking the plasma samples with dosage of VEGF, histamine and TNFα. After incubation with these permeability factors, the microvessels lost their leak-tightness (Figure 4a-c). Although the effect was weak due to protective factors in plasma that maintain the hemostasis conditions of the microvessels, the barrier permeability progressively increased as the concentrations of

VEGF, histamine and TNFα increased. Our findings were also validated with the ECIS system. In this system, VEGF, histamine and TNFα spiked in EDTA-plasma effectively decreased the endothelial barrier function (Figure 4d-f). This corroborates with the increased vessel permeability seen in the microvessels-on-chips. Importantly, the increased barrier permeability was associated with the formation of stress fibers and rearrangement of VE-cadherin (Figure 4g). Incubation with TNFα also induced the expression of tissue factor (Figure 4h).

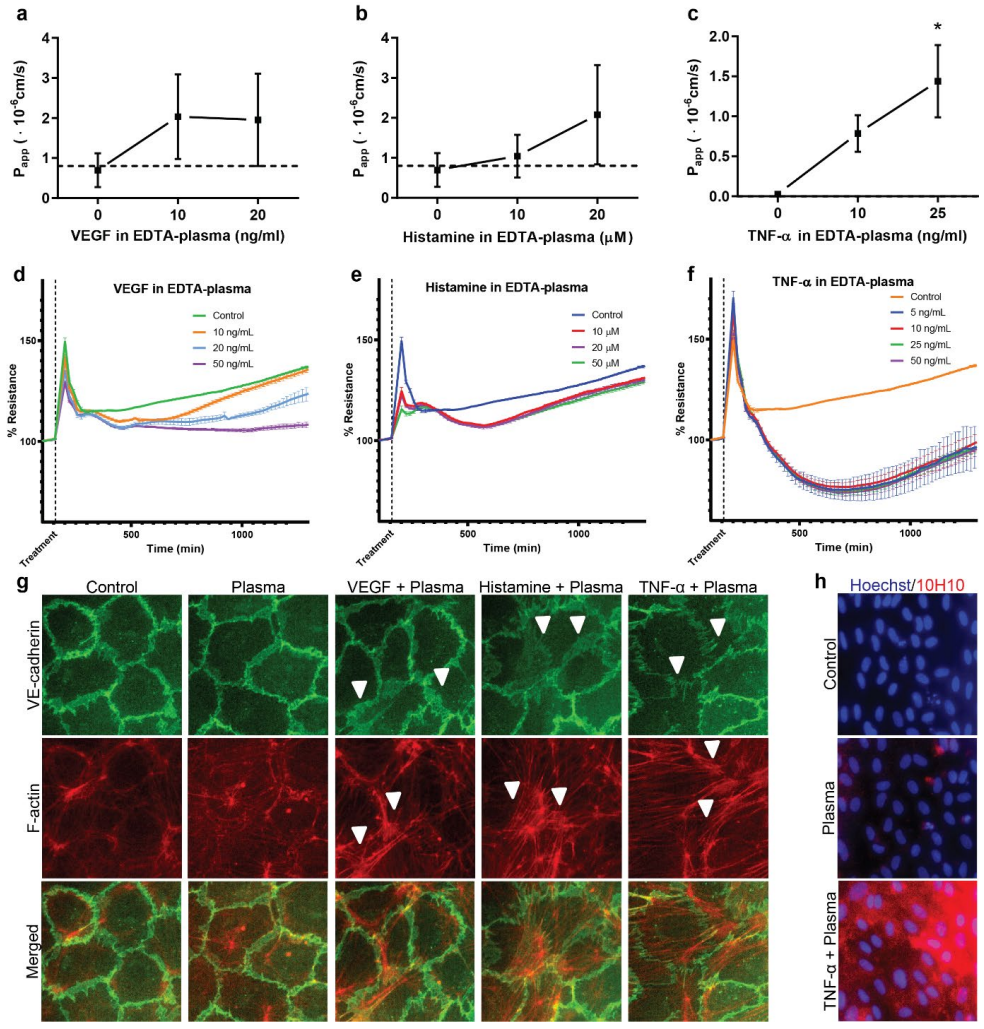

Figure 4 | Permeability effect of perfusing blood plasma in microvessel-on-a-chip. Dose response to **(a)** VEGF (1.5h), **(b)** histamine (1h) and **(c)** TNFα (overnight) spiked at several concentrations in recalcified EDTA-plasma treated with 1 μM hirudin, 50 μg/ml CTI and 25 μM compstatin. Data are presented as mean and s.e.m of two biological replicates; n = 6 (chips). Significance determined by ANOVA and Dunnett's t-test; *P < 0.05. **(d-f)** The effects of VEGF, histamine and TNFα spiked in recalcified EDTA-plasma on endothelial barrier function were measured in the Electric Cell-substrate Impedance Sensing (ECIS) at different doses. Data are represented as mean and s.e.m of 3-4 technical replicates. **(g)** Immunostaining of endothelial cells for nucleus (blue), VE-cadherin (green) and F-actin (red) after treatment with 10 ng/ml VEGF (1.5h), 10 μM histamine (1h) and 10 ng/ml TNFα (overnight) spiked in recalcified EDTA-plasma treated with hirudin, CTI and compstatin. In both conditions an increase in actin stress fiber formation (arrowheads) and morphological arrangement of VE-cadherin were

observed. **(h)** Immunofluorescence for nucleus (blue) and tissue factor expression (red) after treatment with 10 ng/ml TNFα spiked in recalcified EDTA-plasma containing hirudin, CTI and compstatin (overnight).

Discussion

Despite progress in identifying critical regulators of endothelial permeability, it is not fully clear how certain factors in blood induce an impaired endothelial barrier. In this work, we introduced a unique approach using a microfluidic-based *in vitro* assay, microvessel-on-a-chip, that enabled parallel culture, real-time visualization and parallel quantification of endothelial permeability. We showed that VEGF, histamine and TNFα modulate the endothelial barrier. This is also consistent with *in vivo* observations, highlighting the potential of the microvessels-on-chips to study vessel permeability factors in blood [23-25].

Compared to traditional 2D-based assays, the microvessels-on-chips allows us to add physiological relevant cues to the vasculature *in vitro* with several advantages. For example, cell-cell and cell-ECM interaction and perfusion are considerably reduced in 2D cell culture, which in turn significantly limits their ability to mimic the appropriate level of *in vivo* cellular responses. With the microvessels-on-chips we could breach the gap between *in vitro* 2D cell culture and *in vivo* models, enabling us to accurately predict *in vivo* permeability. Furthermore, in our high-throughput platform we are dealing with low volume samples. This gives the possibility to do multiple experiments in a cost effective manner.

Previous studies of endothelial permeability with microfluidic-based approaches were largely done by perfusing cell culture media in the system [26-28]. However, we developed a novel method to directly screen vascular diseases by using primary endothelial cells and blood. In this procedure, we extracted plasma from blood, treated it and perfused it in the cultured human microvessels. To prevent blood plasma from clotting, we primarily inhibited thrombin. This was not only to prevent coagulation induced by recalcification, but also to block the expression of tissue factor that turns on procoagulant activity at the cell surface during vascular diseases [29]. Next to that, due to the negative charge surface of the microchannels of the OrganoPlate, we inhibited the intrinsic pathway of coagulation. This also inhibits the classical pathway of complement activation, since Factor XIIa and kallikrein are known to cleave C1s [30]. Besides preventing clotting, the release of bradykinin, a proinflammatory

peptide that increase endothelial permeability, is suppressed [31]. Considering these factors, there might be crosstalk between the coagulation and complement systems in vascular diseases that can further be intercepted with anti-coagulants and complement inhibitors [32].

The microvessels-on-chips permitted high-throughput stimulation of the vascular permeability induced by our EDTA-plasma cocktail when spiked with VEGF, histamine and TNFα. This vessel permeability was confirmed with TEER measurements by using the ECIS system. However, TEER values vary significantly due to biological and environmental factors, thereby making endothelial cells very sensitive to cytokines and growth factors. On the other hand, the microvessels-on-chips, as a 3D culture system, is a closed system with excellent control and standardization of prepared microvessels with stable endothelial cells [33, 34]. This might have resulted in the reduced permeability effect seen in our platform with greater resemblance to *in vivo* tissue-like physiological responses [35]. Therefore our findings can be applied to disease treatment, where early diagnosis is necessary to properly manage the disease and develop the pharmacokinetic modelling of drug treatments, as initiation of rapid therapy is key to reducing deaths.

Overall, the microengineered human microvessels-on-chips faithfully recapitulated the physiology and pathology of microvessels *in vivo* that can aid as a sensing platform in clinical trials. This offers the possibility to be used as a “disease-on-a-chip” for carrying out cardiovascular studies on drug toxicity *in vitro* as well as dissecting the molecular mechanisms that mediate this process.

Conflict of interest

Authors declare no conflict of interest related to the content of this manuscript.

Acknowledgments

AJ, JvG, TH and AJvZ were financially supported by the RECONNECT CVON Groot consortium, which is funded by the Dutch Heart Foundation.

References

1. Mozaffarian, D., et al., *Executive Summary: Heart Disease and Stroke Statistics-2016 Update A Report From the American Heart Association.* Circulation, 2016. **133**(4): p. 447-454.

2. Rabelink, T.J., H.C. de Boer, and A.J. van Zonneveld, *Endothelial activation and circulating markers of endothelial activation in kidney disease.* Nature Reviews Nephrology, 2010. **6**(7): p. 404-414.

3. Mestas, J. and C.C.W. Hughes, *Of mice and not men: Differences between mouse and human immunology.* Journal of Immunology, 2004. **172**(5): p. 2731-2738.

4. McGonigle, P. and B. Ruggeri, *Animal models of human disease: Challenges in enabling translation.* Biochemical Pharmacology, 2014. **87**(1): p. 162-171.

5. van Esbroeck, A.C.M., et al., *Activity-based protein profiling reveals off-target proteins of the FAAH inhibitor BIA 10-2474.* Science, 2017. **356**(6342): p. 1084-1087.

6. Benam, K.H., et al., *Small airway-on-a-chip enables analysis of human lung inflammation and drug responses in vitro.* Nature Methods, 2016. **13**(2): p. 151-+.

7. Wevers, N.R., et al., *High-throughput compound evaluation on 3D networks of neurons and glia in a microfluidic platform.* Scientific Reports, 2016. **6**.

8. Ramadan, Q. and F.C.W. Ting, *In vitro micro-physiological immune-competent model of the human skin.* Lab on a Chip, 2016. **16**(10): p. 1899-1908.

9. Trietsch, S.J., et al., *Membrane-free culture and real-time barrier integrity assessment of perfused intestinal epithelium tubes.* Nature Communications, 2017. **8**.

10. Zervantonakis, I.K., et al., *Three-dimensional microfluidic model for tumor cell intravasation and endothelial barrier function.* Proceedings of the National Academy of Sciences of the United States of America, 2012. **109**(34): p. 13515-13520.

11. Zhang, B., et al., *Biodegradable scaffold with built-in vasculature for organ-on-a-chip engineering and direct surgical anastomosis.* Nat Mater, 2016. **15**(6): p. 669-78.

12. Deosarkar, S.P., et al., *A Novel Dynamic Neonatal Blood-Brain Barrier on a Chip.* PLoS One, 2015. **10**(11): p. e0142725.

13. Junaid, A., et al., *An end-user perspective on Organ-on-a-Chip: Assays and usability aspects.* Current Opinion in Biomedical Engineering, 2017. **1**: p. 15-22.

14. Paulus, W.J. and C. Tschope, *A Novel Paradigm for Heart Failure With Preserved Ejection Fraction Comorbidities Drive Myocardial Dysfunction and Remodeling Through Coronary Microvascular Endothelial Inflammation.* Journal of the American College of Cardiology, 2013. **62**(4): p. 263-271.

15. Briet, M. and K.D. Burns, *Chronic kidney disease and vascular remodelling: molecular mechanisms and clinical implications.* Clinical Science, 2012. **123**(7-8): p. 399-416.

16. Ulker, E., et al., *Ascorbic acid prevents VEGF-induced increases in endothelial barrier permeability.* Molecular and Cellular Biochemistry, 2016. **412**(1-2): p. 73-79.

17. Park-Windhol, C. and P.A. D'Amore, *Disorders of Vascular Permeability.* Annual Review of Pathology: Mechanisms of Disease, Vol 11, 2016. **11**: p. 251-281.

18. Ashina, K., et al., *Histamine Induces Vascular Hyperpermeability by Increasing Blood Flow and Endothelial Barrier Disruption In Vivo.* Plos One, 2015. **10**(7).

19. Schaefer, A., et al., *Endothelial CD2AP Binds the Receptor ICAM-1 To Control Mechanosignaling, Leukocyte Adhesion, and the Route of Leukocyte Diapedesis In Vitro.* Journal of Immunology, 2017. **198**(12): p. 4823-4836.

20. Kidoya, H., H. Naito, and N. Takakura, *Apelin induces enlarged and nonleaky blood vessels for functional recovery from ischemia.* Blood, 2010. **115**(15): p. 3166-3174.

21. Lindorfer, M.A., et al., *Compstatin Cp40 blocks hematin-mediated deposition of C3b fragments on erythrocytes: Implications for treatment of malarial anemia.* Clinical Immunology, 2016. **171**: p. 32-35.

22. Zhang, Y.Z., et al., *Compstatin analog Cp40 inhibits complement dysregulation in vitro in C3 glomerulopathy.* Immunobiology, 2015. **220**(8): p. 993-998.

23. Kobayashi, K., et al., *Thromboxane A2 exacerbates acute lung injury via promoting edema formation.* Sci Rep, 2016. **6**: p. 32109.

24. Jiang, S., et al., *Vascular endothelial growth factors enhance the permeability of the mouse blood-brain barrier.* PLoS One, 2014. **9**(2): p. e86407.

25. Lundeberg, E., et al., *Assessing Large-Vessel Endothelial Permeability Using Near-Infrared Fluorescence Imaging-Brief Report.* Arteriosclerosis Thrombosis and Vascular Biology, 2015. **35**(4): p. 783-786.

26. Phan, D.T.T., et al., *A vascularized and perfused organ-on-a-chip platform for large-scale drug screening applications.* Lab Chip, 2017. **17**(3): p. 511-520.

27. Ryu, H., et al., *Engineering a Blood Vessel Network Module for Body-on-a-Chip Applications.* J Lab Autom, 2015. **20**(3): p. 296-301.

28. Maoz, B.M., et al., *A linked organ-on-chip model of the human neurovascular unit reveals the metabolic coupling of endothelial and neuronal cells.* Nat Biotechnol, 2018. **36**(9): p. 865-874.

29. Rao, L.V.M. and U.R. Pendurthi, *Regulation of tissue factor coagulant activity on cell surfaces.* Journal of Thrombosis and Haemostasis, 2012. **10**(11): p. 2242-2253.

30. Gorbet, M.B. and M.V. Sefton, *Biomaterial-associated thrombosis: roles of coagulation factors, complement, platelets and leukocytes.* Biomaterials, 2004. **25**(26): p. 5681-703.

31. Ehringer, W.D., M.J. Edwards, and F.N. Miller, *Mechanisms of alpha-thrombin, histamine, and bradykinin induced endothelial permeability.* Journal of Cellular Physiology, 1996. **167**(3): p. 562-569.

32. Lupu, F., et al., *Crosstalk between the coagulation and complement systems in sepsis.* Thrombosis Research, 2014. **133**: p. S28-S31.

33. Ghaffarian, R. and S. Muro, *Models and methods to evaluate transport of drug delivery systems across cellular barriers.* J Vis Exp, 2013(80): p. e50638.

34. van Duinen, V., et al., *96 perfusable blood vessels to study vascular permeability in vitro.* Scientific Reports, 2017. **7**(1): p. 18071.

35. Lee, J., et al., *In vitro Toxicity Testing of Nanoparticles in 3D Cell Culture.* Small, 2009. **5**(10): p. 1213-1221.

36. Vulto, P., et al., *Phaseguides: a paradigm shift in microfluidic priming and emptying.* Lab on a Chip, 2011. **11**(9): p. 1596-1602.

37. Huxley, V.H., F.E. Curry, and R.H. Adamson, *Quantitative Fluorescence Microscopy on Single Capillaries - Alpha-Lactalbumin Transport.* American Journal of Physiology, 1987. **252**(1): p. H188-H197.

38. van Duinen, V., et al., *96 perfusable blood vessels to study vascular permeability in vitro.* Scientific Reports, 2017. **7**.

Supplementary Figures

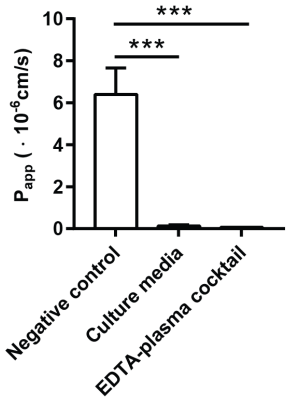

Supplementary Figure 1 | Permeability of empty microchannels (negative control), microvessels perfused with culture media and EDTA-plasma cocktail (recalcified 50% EDTA-plasma with 1 μM hirudin, 50 μg/ml CTI and 25 μM compstatin). Data are presented as mean and s.e.m; n = 4-17 (chips). Significance determined by ANOVA and Dunnett's t-test; ***P < 0.001.